International Journal of Multiphysics
Volume 18, No. 2, 2024
ISSN: 1750-9548

Rapid Fault Diagnosis and Location Technique of Overhead Line based on Quantum Algorithm Optimization

Jiang Hao*[1], Zhang Boxian[2], Sun Ranran[3], Qian Yining[4]

1.Electrical Engineering， State Grid Zhejiang Electric Power Co., Ltd. Ningbo Power Supply Company, Ningbo 315000, China

2.distribution automation and network security， State Grid Zhejiang Electric Power Co., Ltd. Ningbo Power Supply Company, Ningbo 315000, China

3.distribution automation technology, distribution network technology，State Grid Zhejiang Electric Power Co., Ltd. Ningbo Power Supply Company, Ningbo 315000, China

4.Distribution Network Technology, Distribution Automation Technology，State Grid Zhejiang Electric Power Co., Ltd. Ningbo Power Supply Company, Ningbo 315000, China

Corresponding author*，Email：15988644828@163.com

Abstract

An innovative approach for diagnosing the kind and phase of faults on overhead transmission lines (OHTLs) is presented in this research. Quantum-centric galactic search optimized support vector regression (QGSO-SVR) is proposed in this work for an effective fault detection process. Data instances, or signals, are obtained at the transmitting and receiving portions of the line to evaluate the effectiveness of the suggested method. Principal component analysis (PCA) is used to identify the important features from the raw data after wavelet transform (WT) has been used to reduce the signal's volume of data without compromising the detection accuracy. The suggested model is trained using frequencies across various fault regions. Further improvements are made to the SVR's fault detection technique according to quantum characteristics in the galactic optimization procedure. Estimating the location of the defect comes after identifying the faulty phase or phases. The suggested approach is used to analyze effectiveness regarding speed and precision using the Matlab tool. Extensive simulation was conducted for different levels of fault resistances (FR), inception angles, and positions. It was researched how noise affects the current and voltage measurements. Based on the analysis of the experiments, the proposed approach has provided 267.85 km in speed which seems to be the best technique for identifying fault diagnosis and location of overhead line.

Keywords- Overhead transmission line (OHTL), voltage, frequency component, fault diagnosis, fault location (FL), Quantum-centric galactic search optimized support vector regression (QGSO-SVR)

1. Introduction

Identifying, categorizing, and locating transmission-line defects are the three main responsibilities involved in transmission-line relays. Transmission-line defects can be quickly separated from service and thereby shielded from

the fault's negative impacts of rapid fault detection [1]. The process of classifying faults includes the identifying type of fault, which is necessary to locate the issue and determine the amount of maintenance that has to be done. In today's power transmission networks, an accurate, quick, and dependable fault categorization method is essential for proper functioning. However, accurate information on the type of defect is easily required for estimating its location. These demands have led to an extensive amount of investigation being done on the issue of developing an accurate fault categorization method [2].

One of the most prominent components of a power distribution structure is the transmission line (TL). They are susceptible to problems because they are exposed to extreme and unanticipated environmental factors [3]. To efficiently and quickly resolve TL challenging zones and minimize the high costs associated with triggering circuit breakers when faults are accidentally found, recognition, identification, and location prediction techniques, such as those based on ML, are crucial. A fault detection system must be able to utilize the small amount of data that it receives in between a fault occurring and the tripping of circuit breakers and relays since tripping relays and circuit breakers become active very quickly [4].

Transmission lines frequently experience short-circuit faults, which are regarded as the most serious type of defect and represent the highest risk to the system. They can reduce components' remaining useful lifetimes, increase power loss and heat at the cables, as well as affect insulators [5]. A wide range of short-circuit defects, mostly categorized as symmetrical or unsymmetrical, develop during daily operations. Triple line-to-ground (LLLG) and triple line (LLL) faults comprise symmetrical or balanced faults, which maintain system stability. Although they are less common, they are the most serious types of short-circuit problems because of their significant impact and potential to damage system components. The line-to-ground (LG), line-to-line (LL), and double line-to-ground (LLG) faults are the asymmetrical or unbalanced faults that lead the electricity system to become imbalanced during the fault [6].

Faster and more accurate fault detection, recognition, and localization significantly enhance the system's maintenance and protection approaches and assist in maintaining power systems' quantity and quality efficiency. The effects of a problem on the system depend upon its nature, location, and duration. The system's signals, including currents, voltages, and rotor angles, will experience temporary changes in phase, frequency, and amplitude during short-circuit problems, depending on the fault type and region. To differentiate between them and other problems, their temporal patterns offer a collection of covariate variables that may be obtained from the signals [7].In this study, a quantum-centric galactic search optimized support vector regression (QGSO-SVR) is presented for an efficient fault identification approach.

The paper's organization is as follows: Related works, methodology, results, and conclusion.

2. Related works

A novel CNF approach for locating and classifying multiple fault types on power transmission lines was presented in the paper [8]. The results revealed that the CNF could capture a wide range of fault conditions, suggesting a shorter period of technical management's time. To avoid fire, an AI-based approach for detecting open conductor faults on overhead cables was suggested in this study [9]. The falling open conductor line connection to the earth was intended to be the source of the system's design fault. The method for the non-intrusive evaluation of high-voltage electrical systems was completed and presented in the study [10]. The approach depends on the application of ML and FRA, which was modeled by a neural classifier developed on an MVN neural network. The simulation findings showed that it was possible to categorize the joints' condition and avoid major problems.

The generation of power in between AC networks could be simulated by using a voltage source converter-based HVDC transmission network, as investigated in [11]. Evaluation could involve ideal and undesirable situations. A medium-volt overhead line with a CC fault identification technique using BLSTM was presented in the research

[12]. The acquired experimental findings demonstrated the superior efficacy of the suggested BLSTM approach in learning the chaotic PD structure. To identify PD signal trends and predict possible failures, the study [13] proposed a methodology that applied ML techniques. Their research approach showed a high percentage of accuracy in the identification of PD fluctuations.

Semantic segmentation was employed in the research [14] to provide an automatic diagnostic approach for overheating issues in OHTL. Such an intelligent detection method was proposed that achieved an accuracy of 91. 0% diagnostic accuracy in measuring the condition of lead wires or strain clamps. A novel strategy and conceptual process for the continuous evaluation, forecasting, and fault identification of the different joint areas of overhead lines for power transfer were provided in the study [15]. The methods were based on approaches to soft computing, ML, and FRA. The suggested approach could be described as an intelligent measurement component, where essential data for the evaluation of a complicated electrical structure could be obtained by a neural processor from a single measurement. The BPNN has been used in the study [16] to build a method for the identification and categorization of OHTL faults. The results indicated that the LM algorithm performs better than both BR and SCG.

3. Methodology

In this study, we gather the dataset with FL, FR, and fault inception angle features. The features are extracted from the collected data using PCA. Then WT is employed to reduce the signal's volume of data. The quantum-centric galactic search optimized support vector regression (QGSO-SVR) is used for an effective overhead line fault identification approach.

3.1 Principal Component Analysis

PCA is a popular dimensionality reduction approach for analyzing information and compression. It operates by identifying a limited number of orthogonal linear combinations of the initial variables with the highest variance, thereby reducing the number of associated variables to a lower number. In the modification, the linear mixture of the initial variables with the highest variance is the initial principal component; the linear mixture of the initial variables with the subsequent largest variance, orthogonal to the initial principal component, is the subsequent principal component, and so on. When data dimensions are reduced, the first few principal components in many data sets represent most of the differences in the initial data set, allowing the remaining portion to be ignored with the least amount of variance loss. The transition proceeds as follows:

Given a collection of observations$w_1, w_2, \dots \dots, w_m$, the data collection is expressed by a matrix n, where every observation is expressed by a vector of length $W_{m\times n}$.

$$W_{m\times n} = \begin{bmatrix} w_{11} & \cdots & w_{1n} \\ w_{21} & \cdots & w_{2n} \\ \cdots & \cdots & \cdots \\ w_{m1} & \cdots & w_{mn} \end{bmatrix} = [w_1, \cdots, w_m] \qquad (1)$$

The average observation is described as

$$\mu = \frac{1}{m}\sum_{j=1}^{m} w_j \qquad (2)$$

The difference from the average is defined as

$$\Phi_j = w_j - \mu \qquad (3)$$

The sample CM of the data set can be described as

$$D = \frac{1}{m}\sum_{j=1}^{m}(w_j - \mu)(w_j - \mu)^S = \frac{1}{m}\sum_{j=1}^{m}\Phi_j\Phi_j^S = \frac{1}{m}BB^S \quad (4)$$

Where$B = [\Phi_1, \Phi_2, \cdots \Phi_m]$.

To determine the eigenvalues and associated eigenvectors of the CM sample D using PCA, the SVD approach is usually employed. Consider that the CMsample$D$ has pairs of eigenvalues and eigenvectors$(\lambda_1, v_1), (\lambda_2, u_2), \ldots\ldots, (\lambda_n, v_n)$ vn, and$n$. The l eigenvectors with the greatest eigenvalues are the ones we choose. There are frequently significant eigenvalues, which suggests that the remaining $(n - l)$ dimensions are typically filled with noise and that l is the intrinsic dimensionality of the subspace regulating the signal. The dimensions of subspace k can be evaluated.

$$\frac{\sum_{j=1}^{l} \lambda_j}{\sum_{j=1}^{n} \lambda_j} \geq \alpha (5)$$

Whereαrepresents the proportion of subspace variation to the overall variation in the initial space. We create a $n \times l$ matrix V with l eigenvectors as its columns.Expressing the data into the l-dimensional subspace is the process of representing the data by principal components.

$$z_j = V^S\left(w_j - \mu\right) = V^S \Phi_j (6)$$

3.2 Wavelet Transform

A sequence of low-pass and high-pass filters is used in the wavelet transform method, a signal processing technique, to separate power signals into distinct frequency ranges to identify abnormal operating circumstances. This yields a time-frequency multi-resolution evaluation, which is very helpful in locating any rapid or sudden changes in electrical parameters like frequency, current, phase, voltage, etc. The fault identification evaluation in the present instance uses Daubechies4 (dB4) as the mother wavelet basis function. The signal is often separated into a set of detail (c) and approximate (b) coefficients, which correspond to the high and low-frequency bands, respectively.

The CWT, given a voltage signal $U(s)$ from the power supply, is described as

$$CWT(U, N, M) = \frac{1}{\sqrt{b}} \int_{-\infty}^{\infty} U(s)^{\Psi^*} \left(\frac{s - M}{N}\right) ds \quad (7)$$

The wavelet basis function is denoted by Ψ, and the dilation and translation variables are denoted by N and M. Finally, WT in the discrete form as,

$$DWT(U, N, M) = \frac{1}{\sqrt{N_0^n}} \sum_l U(l)^{\Psi^*} \left(\frac{m - lN_0^n}{N_0^n}\right) (8)$$

N and M are substituted with N_0^n and lN_0^n, respectively, and l is a single integer. The scaling function in the initial phase is represented as the sum of the subsequent phase andit could be expressed as follows,

$$\varphi(s) = \sum_{m=-\infty}^{\infty} g(m) \sqrt{2} \varphi(2s - m) (9)$$

The primary voltage signal can be expressed through the previous equation.

$$U(s) = \sum_{l \to \infty}^{\infty} b_{op}(l) 2^{\frac{op}{2}} \phi(2^{op} s - l) + \sum_{l=-\infty}^{\infty} \sum_{o=op}^{\infty} c_o(l) 2^{\frac{o}{2}} \phi(2^o s - l) (10)$$

oprepresents the scaling function's coarse modification parameter. The detail and approximate coefficients are expressed as follows,

$$b_o(l) = \sum_{n=-\infty}^{\infty} b_{o+1}(n) g(n - 2l) (11)$$

$$c_o(l) = \sum_{n=-\infty}^{\infty} d_{o+1}(n) g_1(n - 2l) (12)$$

3.3 QGSO-SVR

In this study, the QGSO approach is integrated with SVR which provides QGSO-SVR for the effective fault diagnosis in the overhead lines.

3.3.1 QGSO

QGSO consists of the principles of quantum bit and rotation gate, it also offers a greater search capability and a faster rate of convergence.Unlike a galaxy's velocity and location in the conventional GSO, a galaxy's state is represented by a quantum bit and angle in the QGSO. We define these terms below.

- A pair of numbers is a description of a quantum bit, which is the smallest component in the QGSO.

$$\begin{bmatrix}\alpha_{ij}(x)\\ \beta_{ij}(x)\end{bmatrix},\ \begin{cases} i = 1,2,\dots\dots,n \\ j = 1,2,\dots\dots,m \end{cases} \tag{13}$$

The possibility that the quantum bit is present in states 0 and 1 is given by the modulus $\left|\alpha_{ij}(x)\right|^2 and \left|\beta_{ij}(x)\right|^2$, correspondingly, and they must be satisfied.

$$\left|\alpha_{ij}(x)\right|^2 + \left|\beta_{ij}(x)\right|^2 = 1 \tag{14}$$

A quantum bit individual, which is the component that comprises a string of quantum bits, is described as

$$r_i(x) = \begin{bmatrix}\alpha_{i1}(x),\dots\dots,\alpha_{ij}(x),\dots\dots,\alpha_{im}(x)\\ \beta_{i1}(x),\dots\dots,\beta_{ij}(x),\dots\dots,\beta_{im}(x)\end{bmatrix} = \left[r_{i1}(x),\dots.,r_{ij}(x),\dots.,r_{im}(x)\right] \tag{15}$$

The probability description of a quantum bit allows it to express a linear combination of every potential outcome. Consequently, combinations of various quantum bit levels can be used to describe completely 2^m types of individuals. Compared to other descriptions, this quantum bit structure is more effective at producing population variety. For example, if three quantum bit individuals with two pairs of amplitudes exist, such as

$$\begin{bmatrix}\frac{1}{\sqrt{2}} & \frac{1}{2} & \frac{1}{\sqrt{2}}\\ \frac{1}{\sqrt{2}} & \frac{\sqrt{3}}{2} & \frac{-1}{\sqrt{2}}\end{bmatrix} \tag{16}$$

Subsequently, the individual's positions can be shown as

$$\left\{\frac{1}{4}|000\rangle,\frac{-1}{4}|001\rangle,\frac{\sqrt{3}}{4}|011\rangle\frac{1}{4}|100\rangle,\frac{-1}{4}|101\rangle,\frac{\sqrt{3}}{4}|110\rangle,\frac{-\sqrt{3}}{4}|111\rangle\right\} \tag{17}$$

The probability that represents the various states, 0 or 1, is indicated by the above outcome. The information of eight distinct states can be found in a single quantum bit.

- The normalization criteria allow for the representation of the quantum angle as

$$\begin{cases}\left|r_{ij}(x)\right\rangle = cos\theta_{ij}(x)\left|0\right\rangle + sin\theta_{ij}(x)|1\rangle \\ \theta_{ij}(x) = arctan\frac{\beta_{ij}(x)}{\alpha_{ij}(x)}\end{cases} \tag{18}$$

The quantum angle can be utilized for representing the individual quantum bit.

$$\begin{array}{cccc} \vec{r}_i(x) = & [r_{i1}(x), \ldots\ldots, . & r_{ij}(x), \ldots\ldots & r_{im}(x)] \\ \downarrow & \downarrow & \downarrow & \downarrow \\ \theta_i(x) = & \theta_{i1}(x), \ldots\ldots, & \theta_{ij}(x), \ldots\ldots, & \theta_{im}(x)] \end{array} \quad (19)$$

Quantum bits and angles are changed because of the basic QGSO updating process, and the modified quantum bits still have to satisfy the normalization criteria. One might calculate the quantum rotational gate updating equation using,

$$\Delta\vec{\theta}_i(x+1) = \omega.\Delta\vec{\theta}_i(x) + \varphi.q_1.\left[\vec{\theta}_{pb} - \vec{\theta}_i(x)\right] + \eta.q_2.\left[\vec{\theta}_{gb} - \vec{\theta}_i(x)\right] \quad (20)$$

Whereω is the inertia weight ($\omega = 0.72$)φ, η represents the parameters (i.e. $\varphi = 1.65, \eta = 1.81$), the random numbers$q_1 and q_2$are in the range (0, 1), $\Delta\vec{\theta}_i(\cdot)$ is the change of the angle,$\vec{\theta}_i(\cdot)$ represents the present angle, $\vec{\theta}_{pb}, and\vec{\theta}_{gb}$ represents the local and global best angles.

However having superior population diversity features, premature convergence problems may still arise with the quantum bit and rotation gate model. Concentration and affinity are the two quality barriers that emerge after we identify the global best individual in the evolutionary process and assume that it remains unchanged over iterations.The concentration shows the percentage of quantum individuals in the existing population, while the affinity value represents the quality of a particular individual to the problems.

3.3.2 Support Vector Regression (SVR)

A non-linear MF is used to transform the initial IS, which is typically non-linearly connected to the predictor variable, onto an FS with greater dimensions to handle these irregularities. This is a basic concept for the SVR. The regression issue will be solved using the FS, which is specifically encoded in the kernel matrix, as an additional IS.

Let $H(M \times N)$ be the data set and $z_j \in Q$ be the output vector. Using the provided data set T as a basis, SVR attempts to identify a multivariate regression function $e(h)$ that would forecast the intended output characteristic of an unidentified object. A thorough description of the SVR equations is provided. As a result, we will express the SVR equation as follows,

$$e(h) = \sum_{j,i=1}^{M}\left(\propto_j - \propto_j^*\right)\langle\phi\left(h_j\right).\phi(h_i)\rangle + a \quad (21)$$

Where D is a regularization constant that establishes a balance between the training error and model effectiveness, and $\propto_j and \propto_j^*$ represents the LM achieving constraint $0 \leq \propto_j, \propto_j^* \leq D$. The initial position of the regression function $e(h)$ is represented by parameter a, and the MF is represented by component ϕ. It is challenging to identify the non-linear mapping $\phi(h)$ because it is typically unknown previously. Frequently, a KF is used to calculate the mapping term $\langle\phi(h_j)\phi(h_i)\rangle$ in Equation (22).

$$L\left(h_j, h_i\right) = \langle\phi\left(h_j\right).\phi(h_i)\rangle \quad (22)$$

We can easily managethe non-linear interactions in the data according to this kernel modification. Variance–covariance, polynomial, RBF–based kernels, PUK, and RBF are among the KFs that are appropriate to handle non-linear regression issues. We have demonstrated that the PUK KF may act as a general substitute for the polynomial, RBF-based KFs, and variance-covariance that are frequently used.

Equation (23) becomes equivalent once the KF is performed,

$$e(h) = \sum_{j,i=1}^{m} (\alpha_j - \alpha_j^*) L(h_j, h_i) + a \quad (23)$$

The non-linear IS is typically transformed through the KF, into a high-dimensional FS where the solution to the issue can be described as a straight linear issue. Through employing QP to solve the altered regression issue, the $\propto_j and \propto_j^*$ values are found. As a result, they are referred to as support vectors since the input objects belonging to the non-zero LM$\propto_j and \propto_j^*$ contribute to the last regression design.

3.3.3 QGSO-SVR

An innovative method for identifying faults and diagnosis for overhead power lines is QGSO-SVR. With the use of GSO and quantum computing concepts, this technique aims to change power transmission systems' fault identification.Particularly in complex network environments, conventional fault diagnostic approaches frequently struggle with accuracy and performance issues. This approach utilizes the huge processing capacity and scalability of quantum systems by including quantum-centric calculations, making fault data evaluation easier and quicker.The technique is made more effective by adding GSO. This optimization approach, influenced by celestial navigation concepts, identifies faults with remarkable accuracy by navigating through large data locations.The model gains improved diagnostic abilities gradually by learning and adapting to different problem circumstances through SVR. This technique leads to a resilient electrical network by reducing delay, improving grid dependability, and precisely diagnosing and localizing faults in overhead power lines.

4. Result

Testing and training datasets were two different sets of parameters used in the study. FL, FR, and fault inception angle (θ) varied among the five fault categories in every data set. The training dataset had fault inception angles of 0 and 90 degrees, whereas the testing dataset had angles of 0 and 45 degrees.Additionally, FRs varied between 0 and 40 Ω in the training set and 0 to 20 Ω in the testing set.While FLs in the testing dataset ranged from 20 to 280 kilometers from the transmitting end, they varied from 10 to 290 kilometers in the training dataset. There were 1200 patterns in the training dataset in total. Whereas the testing dataset included 140 patterns that represented the same fault categories with slightly fewer parameter variations.

A $400\ kV$, 50 Hertz, three-phase power system network was created using MATLAB-7 Simpower Toolbox, which is displayed in Figure 1. The balanced load's parameters are listed below in Table 1.

Table 1: Balanced load parameters

Parameter	Value
Transmission cable length	$300\ km$
Power factor $(P.f.)$	0.9
MVA rating	200
Load impedance	$720 + j11\ \Omega$

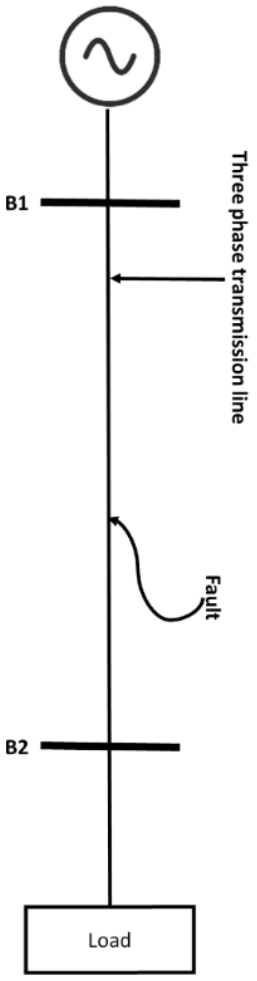

Figure 1: Three-phase network's single-line design

Each signal has a sample time of 78.28 μs, and MATLAB has allowed for a simulation duration of up to 0.04 sec. There are 12.8 kHz of sampling frequency. This system simulates the five kinds of faults listed below.

- single-line-ground fault corresponding to stages B, C, and AareBG, CG, and AG;
- double-line faults such as BC, CA, andAB;
- double-line–ground fault such asCAG, ABG, and BCG;
- Three-phase fault namely LLL.

Every defect has originated at 14 distinct locations, starting with B1, which is12 km apart.Using MATLAB simulation, this noise has been introduced into the training data, which consists of 140 elements in total.

The location and FR statistics for the various fault categories (CG, AG, BC, ABG, and CAG) at different distances are shown in Figure 2. For instance, for an FR of 0 Ω, the actual FL of AG is reported as around 260 kilometers, our proposed method achieved the predicted distance is 267.85 kilometers. With an FR of 0 Ω, the actual FL of CG is around 20 km, although our QGSO-SVR obtained the predicted value indicates a distance of 20.72 kilometers, whereas the actual FL of BC was determined at about 20 kilometers. Our proposed method predicted a value at a location of 20.56 kilometers. ABG and CAG's actual FL is around 200 kilometers, although the predicted distance to a location of 203.35 km was obtained by QGSO-SVR.

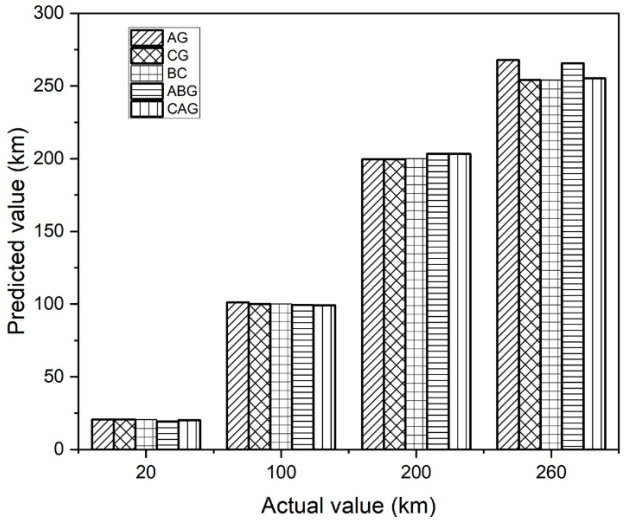

Figure 2: Outcomes of the assessment of FL with 0 FR

Figure 3 displays the location and information on FR for the different fault types (CG, AG, BC, ABG, and CAG) at varying distances. For example, when the FR is equal to 20Ω, the actual AG FL is around 200 kilometers, whereas our proposed method obtained the predicted distance of 207.96 km. The actual FL of CG, with an FR of 20Ω, is approximately 200 km, while the proposed predicted value achieved a distance of 207.35 km. Similarly, the actual FL of ABG was found to be approximately 260 km, while the QGSO-SVR achieved a predicted value of 260.69 km. The actual FL for BC and CAG is considered to be approximately 200 km, despite the anticipated distance being 200.51 km, and 204.05 kilometers were obtained by QGSO-SVR.

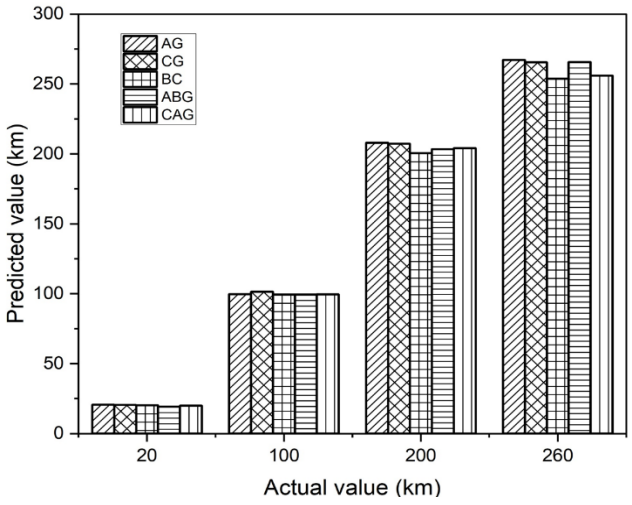

Figure 3: Result of the evaluation of FL with 20 FR

After applying 10 dB of noise, our proposed method achieved the predicted distance of the AG fault of 269.4 km: however, the actual location is approximately 260 km when the FR reaches 0Ω. The actual FL for ABG and CAG is considered to be approximately 200 km, whereas our proposed method achieved the predicted distancesof 206.16 and 204.05 kilometers. Similarly, it was discovered that the actual location of the CG fault was roughly 260 kilometers, although our QGSO-SVR method obtained the predicted distances indicating a location of 269.89 km. With an FR of 0Ω, the actual FL of BC is approximately 20 kilometers. The predicted distance indicates a distance

of 20.90 km was obtained by QGSO-SVR. The findings for fault localization calculations with 10 dB noise applied to the voltage signals are shown in Figure 4.

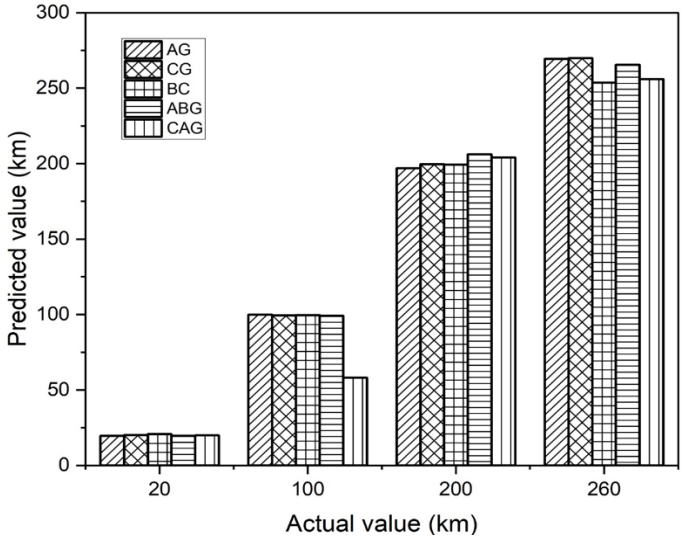

Figure 4: Outcomes of FL with 0 FR after adding 10 Db noises

5. Conclusion

The modern world depends heavily on a steady supply of electricity, and overhead power lines are essential to maintaining that supply. In this study, QGSO-SVR is proposed to effectively identify faults in OHTL. In 0 FR, AG's actual value is 260 kilometers, and our proposed achievedpredicted distance is 267.85 kilometers. Our proposed method reached the predicted distance of 207.96 kilometers, but AG's actual value in 20 FR was 200 kilometers. Our suggestion achieved the predicted distance of 269.4 kilometers after applying 10 dB noises, however, AG's actual value in 0 FR was 260 kilometers. Environmental variables and electromagnetic interference are two instances of noise and instability sources that might affect overhead line systems. QGSO-SVR may not be sufficiently strong to handle various sources of variations, resulting in poor performance in real-world applications. Future developments might concentrate on improving QGSO-SVR to deal with environmental variables and electromagnetic interference in overhead line networks, providing reliable performance in real-world situations.

Reference

1. Venkatesh, V., 2018. Fault classification and location identification on electrical transmission network based on machine learning methods.
2. Padhy, S.K., Panigrahi, B.K., Ray, P.K., Satpathy, A.K., Nanda, R.P. and Nayak, A., 2018, December. Classification of faults in a transmission line using artificial neural network. In *2018 International Conference on information technology (ICIT)* (pp. 239-243). IEEE.
3. Shakiba, F.M., Shojaee, M., Azizi, S.M. and Zhou, M., 2022. Real-time sensing and fault diagnosis for transmission lines. *International Journal of Network Dynamics and Intelligence*, pp.36-47.
4. Kulikov, A., Ilyushin, P., Loskutov, A. and Filippov, S., 2023. Fault Location Method for Overhead Power Line Based on a Multi-Hypothetical Sequential Analysis Using the Armitage Algorithm. *Inventions*, *8*(5), p.123.
5. Zand, M., Nasab, M.A., Padmanaban, S. and Khan, B., 2023. Introducing a New Method for DPMU in Detecting the Type and Location of the Fault. *International Journal of Sensors Wireless Communications and Control*, *13*(5), pp.296-317.

6. Ortega, J.S. and Tavares, M.C., 2019. Transient analysis and mitigation of resonant faults on half-wavelength transmission lines. *IEEE Transactions on Power Delivery*, *35*(2), pp.1028-1037.
7. Benson, U., Jagruti, B., Jadhav, S. and Pawar, B., 2022. Transmission Line Fault Location and Classification Using Machine Learning Technique. *Journal of Recent Trends in Electrical Power System*s, *5*(1), pp.19-33.
8. Pouabe Eboule, P.S. and Hasan, A.N., 2021. Accurate Fault Detection and Location in Power Transmission Line Using Concurrent Neuro Fuzzy Technique. *Przeglad Elektrotechniczny*, *97*(1).
9. Che, J., Kim, T., Pyo, S., Park, J., An, B. and Park, T., 2023. Prevention of Wildfires Using an AI-Based Open Conductor Fault Detection Method on Overhead Line. *Energies*, *16*(5), p.2366.
10. Belardi, R., Bindi, M., Grasso, F., Luchetta, A., Manetti, S. and Piccirilli, M.C., 2020, September. A complex neural classifier for the fault prognosis and diagnosis of overhead electrical lines. In *IOP Conference Series: Earth and Environmental Science* (Vol. 582, No. 1, p. 012001). IOP Publishing.
11. Muzzammel, R., 2019. Machine learning-based fault diagnosis in HVDC transmission lines. In *Intelligent Technologies and Applications: First International Conference, INTAP 2018, Bahawalpur, Pakistan, October 23-25, 2018, Revised Selected Papers 1* (pp. 496-510). Springer Singapore.
12. Ahmad, D. and Wang, S., 2020, July. Bidirectional LSTM-Based Partial Discharge Pattern Analysis for Fault Detection in Medium Voltage Overhead Lines with Covered Conductors. In *2020 IEEE 18th International Conference on Industrial Informatics (INDIN)* (Vol. 1, pp. 70-73). IEEE.
13. Bajwa, B., Butani, C. and Patel, C., 2022. A novel approach towards predicting faults in power systems using machine learning. *Electrical Engineering*, pp.1-6.
14. Yang, X., Tu, Y., Yuan, Z., Zheng, Z., Chen, G., Wang, C. and Xu, Y., 2024. Intelligent overheating fault diagnosis for an overhead transmission line using semantic segmentation. *High Voltage*.
15. Bindi, M., Grasso, F., Luchetta, A., Manetti, S. and Piccirilli, M.C., 2019, November. Smart monitoring and fault diagnosis of joints in high voltage electrical transmission lines. In *2019 6th International Conference on Soft Computing & Machine Intelligence (ISCMI)* (pp. 40-44). IEEE.
16. Teja, O.N., Ramakrishna, M.S., Bhavana, G.B. and Sireesha, K., 2020, September. Fault detection and classification in power transmission lines using back propagation neural networks. In *2020 International Conference on Smart Electronics and Communication (ICOSEC)* (pp. 1150-1156). IEEE.

APPENDIX

OHTL = overhead transmission lines	CNF = concurrent neuro-fuzzy
ML = machine learning	FRA = frequency response analysis
MVN = Multi-Valued Neuron	HVDC = High-voltage direct current
CC = covered conductors	BLSTM = bidirectional long short-term memory
PUK = Pearson VII Universal Kernel	BPNN = Back propagation neural networks
LM = Levenberg-Marquardt	BR = Bayesian Regularization
SCG = Scaled Conjugate Gradient	CM = covariance matrix
SVD = Singular Value Decomposition	FS = feature space
CWT = continuous wavelet transform	LM = Lagrange multipliers
FL = Fault location	KF = kernel function
PD = partial discharge	RBF = Radial Basis Function
QP = quadratic programming	MF = mapping function
IS = input space	